

Electrostatic Charge Evolution of a Falling Droplet Application to Splash Filling

Sylvia Lüttgens¹, Günter Lüttgens¹, Anders Thulin², Thierry Paillat³, Gérard Touchard³

¹ELSTATIK, Odenthal, Germany, ²ATC AB, Saltsjöbaden, Sweden,

³PPRIME Institute, Bd Marie & Pierre Curie, BP30179, 86962 Futuroscope, France.

e-mail: gerard.touchard@univ-poitiers.fr

Abstract –An experimental equipment of around 5m height has been assembled to observe the charge transferred by electrostatic induction of a falling droplet of various liquids during its fall. The droplets were generated by a syringe push with an automat. The droplets can be charged with an applied electric field at the tip of the needle. Then 4 metallic cylinders and a collecting vessel detect the charge on the droplet along its fall. We observe the size of the droplet at the top and the bottom of the fall to be sure that it did not break in several parts.

I. INTRODUCTION

Even if the research report in this paper is purely fundamental, important applications in the field of electrostatic hazards in industry exist. After a website forum on the dangerousness of splash filling with specialists in flow electrification and electrostatic hazards like I. Pavey, M. Glor, U. Von Pidoll, H. Walmsley..., we decided to begin with a fundamental experiment to prove that there is no flow electrification of liquid moving in gas. For that we have examined the evolution of the charge on a droplet falling in air upon a rather long distance. But, first, in order to clearly differentiate the case of a liquid flowing past a solid body and the case of a liquid flowing past a gas, we are going to briefly explain the flow electrification phenomenon and what is found in the case of clean gas flowing past a solid body.

II. FLOW ELECTRIFICATION PHENOMENON

At the contact between a solid and a liquid a physico-chemical process takes place which leads to the formation of a so called Electrical Double Layer. It is a double layer because one part of this layer is in the solid while the second part is in the liquid. Each layer is electrically charged with opposite polarity, this means, for instance, that negative charges are on the solid very close to the interface and in the liquid, on the other side of the interface, positive charges exist. In fact Stern [1] shows that in the liquid two sub-layers exist, one very close to the interface, with a thickness in the order of magnitude of atom diameter, is called the compact layer. A second one, deeper in the liquid can be affected by diffusion, migration and convection; it is called the Diffuse Layer. When the liquid is moving past the solid surface, the compact layer, very close to the interface and strongly connected to it, is not affected by the liquid motion. On the other hand, the diffuse layer, the thickness of which is proportional to the root square of the electrical liquid resistivity is affected by the flow of the liquid especially for high insulating liquids. This phenomenon is now known for a long time and still investigated as it could be at the origin of the so called Electrostatic Hazards [2-3] in various kinds of industries and often give rise to nuisances [4-39]. Even if the charge generation process at the interface is fundamentally different, flow electrification phenomenon exists also for dusty gas flow in pipes [40] and, it is from these experiments and other experiments made in the same domain that it is now clear that flows of clean gas in pipes do not generate flow electrification. Thus, it seems perfectly predictable that a droplet falling in air will not gain electrical charge. However, as no experiments have already clearly demonstrated this fact and as some controversy still exists on the subject, (which could be due to another phenomenon as we will see later), it seems important to make some fundamental investigations on the electrical charge evolution of falling droplets in air.

III. GENERAL EQUATIONS

A falling droplet is submitted to three different forces:

- The gravitation $\vec{F}_g = m g \vec{z}$ (1)

- The buoyant force $\vec{F}_{pA} = -\rho_{air} Vol \vec{z}$ (2)

- The air friction $\vec{D} = -\frac{1}{2} C_D \rho_{air} V^2 A \vec{z}$ (3)

In these equations \vec{F}_g is the force of gravitation, m is the mass of the droplet, g is the gravity constant ($g = 9.81 \text{ m/s}^2$), \vec{z} is the unit vertical vector in down direction, \vec{F}_{pA} is the buoyant force, ρ_{air} is the volumetric mass density of air, Vol is the volume of the droplet, \vec{D} is the force due to the drag, C_D is the drag coefficient, V is the droplet velocity and A the frontal area exposed by the droplet to the flow direction.

Assuming the droplet as a sphere of radius R_a having a volumetric mass density $\rho_{droplet}$ we can write:

$$m = 4/3 \pi R_a^3 \rho_{droplet} \quad (4)$$

and:

$$A = \pi R_a^2 \quad (5)$$

Finally the motion equation is:

$$\gamma = g \left(1 - \frac{\rho_{air}}{\rho_{droplet}} \right) - \frac{3}{8R_a} \frac{\rho_{air}}{\rho_{droplet}} C_D V^2 \quad (6)$$

γ being the droplet acceleration.

An analytical solution exists if we assume C_D constant (which is not the reality, as we will see later).

A. Analytical solution

We put:

$$a = g \left(1 - \frac{\rho_{air}}{\rho_{droplet}} \right) \quad (7)$$

And:

$$b = \frac{3}{8R_a} \frac{\rho_{air}}{\rho_{droplet}} C_D \quad (8)$$

Then, we assume that the droplet has a null velocity at the beginning of its fall, more, the beginning of the fall is taken as the origin of the axis \bar{z} . Thus, we obtain:

$$V = \sqrt{\frac{a}{b}} \tanh(\sqrt{ab} t) \quad (9)$$

It is usual to set:

$$V_M = \sqrt{\frac{a}{b}} \text{ and } T = \frac{1}{\sqrt{ab}} \quad (10)$$

This is the maximum, or limit, velocity that can be reached by the droplet and T a characteristic time.

Finally we obtain:

$$V = V_M \tanh\left(\frac{t}{T}\right) \quad (11)$$

And:

$$z = \frac{1}{b} \text{Ln} \left[\cosh\left(\frac{t}{T}\right) \right] \quad (12)$$

However, even if this analytical solution gives a good idea of the motion of a spherical droplet falling, it is not exact for several reasons. First the drag coefficient C_D is not constant, second the shape of the droplet does not remain spherical, third the proximity of the cylinder influence the droplet motion. We are going to examine these different aspects.

B. Drag coefficient evolution

For very slow motion we have the very well known ‘‘Stokes equation’’:

$$D = 6 \pi \rho_{air} \nu_{air} R_a V \quad (13)$$

Where ν_{air} is the kinematic viscosity of air.

Taking into account equation (3) we find:

$$C_D = \frac{24}{R_e} \quad (14)$$

R_e being the Reynolds number:

$$R_e = \frac{2V R_a}{\nu_{air}} \quad (15)$$

The ‘‘Stokes equation’’ and the equation (14) are available for low Reynolds number, that is to say less than 0.545. For greater Reynolds we take the following analytical law:

$$C_D = \exp \left\{ \left[-1.75863 + 3.16108 \cdot \exp \left(-\frac{\text{Log}_{10}(R_e)}{3.58231} \right) \right] \cdot \text{Ln}(10) \right\} \quad (16)$$

As we can see in figure 1 this analytical expression is in good agreement with experiments of Liebster, Schiller & Schmiedel and Allen after Schlichting [41]

C. The evolution of the shape of a falling droplet

Due to the surface tension, just after it detaches from the needle tip the droplet has a spherical shape, then the pressure applied on the frontal edge by the drag deforms the spherical shape into a kind of ellipsoid in which the vertical diameter is reduced while the horizontal one is enlarged [88-91].

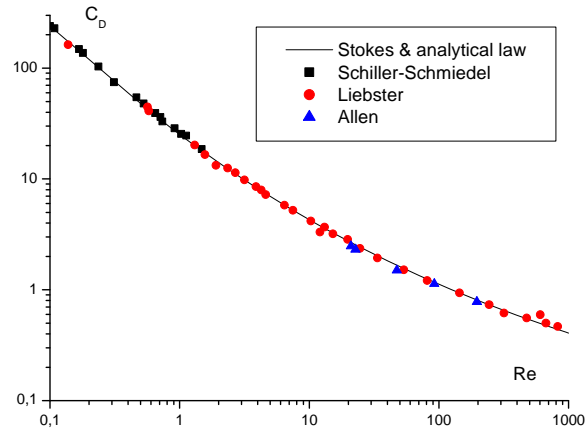


Figure 1 Evolution of the drag coefficient in terms of the Reynolds number up to 1000.

In order to make valuable comparison between predictions and experiments we must take into account this deformation. Thus we made photographs with a high speed camera (Photron Fast Cam APX-RS 1024-1024). An image of a droplet at the nearly end of the fall is shown in figure 2-a. The exposure time is $100 \mu\text{s}$. As we will see later the velocity of the droplet in this zone is around 4.5 m/s , thus it moves around 0.45 mm during $100 \mu\text{s}$. This is noticeable on the photograph. We can see in figure 2-b the photograph simulation of an ellipsoid falling at the same velocity. In figure 2-c we can see this ellipsoid at rest. The horizontal diameter of this ellipsoid is 2 mm and its vertical diameter 1.14 mm ; it seems to be in good agreement with the photograph of the droplet.

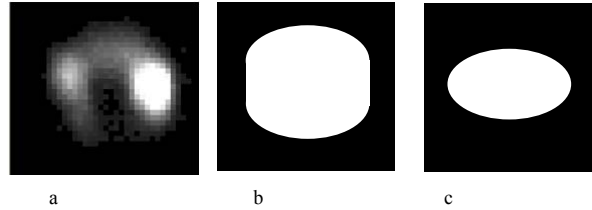


Figure 2 Photograph of the falling droplet (a), equivalent falling ellipsoid (b), ellipsoid (c)

D. Influence of the vicinity of the cylinder

When the droplet falls through the cylinders used to measure the charge transferred by induction as the diameter of these cylinders is smaller than the big cylinder used as a Faraday cage, thus the velocity of the droplet could be influenced by the wall of the cylinders. However, the droplet size is very small compared to the cylinder's diameter then the vicinity of the cylinders can be neglected.

E. Numerical solution

Taking into account the real value of C_D there is no analytical solution of equation (6). Thus, we have to solve numerically the following system of equations:

$$\begin{aligned} \frac{dV}{dt} &= g \left(1 - \frac{\rho_{air}}{\rho_{droplet}} \right) - \frac{3}{8R_a} \frac{\rho_{air}}{\rho_{droplet}} C_D(V) V^2 \\ \frac{dz}{dt} &= V \end{aligned} \quad (17)$$

This system is solved with a Runge-Kutta method of fourth order (RK4). The time increment used is 1 ms (in fact we compared 1 ms increment with 0.5 ms increment and did not find significant difference). By cons, a rather big difference exists between the numerical solution of the exact system (17) with the simplified analytical solution considering the drag coefficient C_D constant and equal to 0.5 as it is usually taken. Indeed, we can see in figure 3 (in the case of a kerosene droplet that we will analyze later) the evolution of the velocity in terms of time of a falling droplet using both methods. As well, in figure 4 is plotted the vertical position of the droplet, we can see that a significant difference exists also.

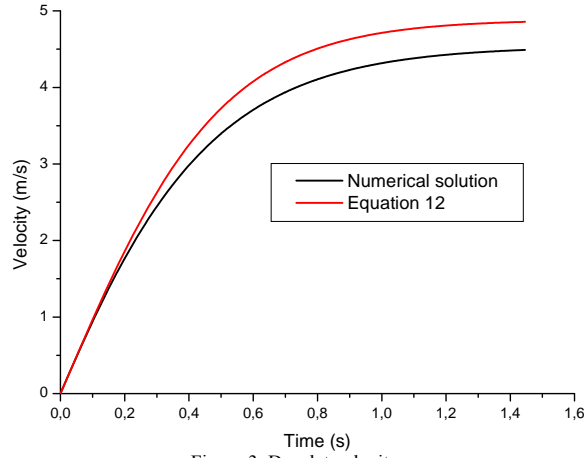


Figure 3. Droplet velocity

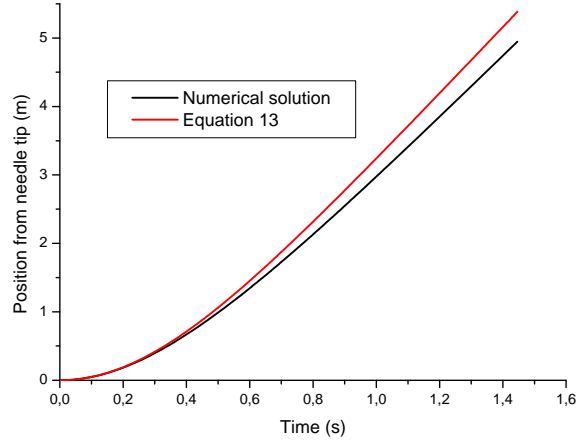


Figure 4. Vertical position of the droplet

Thus, for the evolution of the charge transferred by electrostatic induction by the charged droplet we will consider the results given by the numerical analysis.

IV. CHARGE TRANSFERRED ON SENSORS BY ELECTROSTATIC INDUCTION

As we will see in the setup description, the sensors are composed of 4 vertical cylinders and one collecting vessel all connected together. The collecting vessel in which the droplets are gathered at the end of their fall operates like a Faraday pail; the four successive metallic cylinders are charged by induction from the droplet falling through. To compute the charge induction, we suppose that the charge on the droplet is punctual and that it falls vertically on the cylinder's axis (figure 5). We suppose that the droplet has a charge q_d . If the droplet was totally surrounded by a conductor, the charge induction would be total and the conductor would get the same charge as the droplet (q_d). In that case the solid angle of the cone with its summit at the droplet centre and based on the outline of the conductor is the same that for a total sphere, that is to say 4π (Gauss law). In the case of one cylinder (figure 5) the solid angle Ω is given by the following expression:

$$\Omega = 2\pi [1 - \cos(\alpha_1)] - 2\pi [1 - \cos(\alpha_2)] \quad (18)$$

Finally the charge transferred by electrostatic induction on this sensor, we will suppose it is the cylinder 1 (the upper one), can be written:

$$q_{c1} = \frac{q_d}{2} \{ [1 - \cos(\alpha_1)] - [1 - \cos(\alpha_2)] \} \quad (19)$$

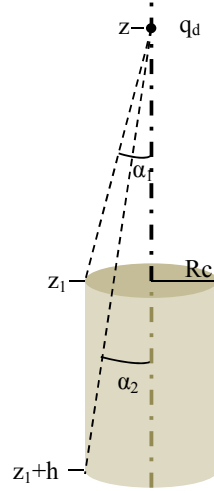


Figure 5. Scheme for the calculus of the charge transferred by electrostatic induction of the droplet in the cylinder.

It can also be written in terms of z (the droplet position), z_1 (the position of the upper side of the cylinder, h (the height of the cylinder) and Rc (the radius of the cylinder).

$$q_{c1} = \frac{q_d}{2} \left[\frac{z_1 + h - z}{\sqrt{(z_1 + h - z)^2 + Rc^2}} - \frac{z_1 - z}{\sqrt{(z_1 - z)^2 + Rc^2}} \right] \quad (20)$$

As well for the three other cylinders we have:

$$q_{c2} = \frac{q_d}{2} \left[\frac{z_2 + h - z}{\sqrt{(z_2 + h - z)^2 + Rc^2}} - \frac{z_2 - z}{\sqrt{(z_2 - z)^2 + Rc^2}} \right] \quad (21)$$

$$q_{c3} = \frac{q_d}{2} \left[\frac{z_3 + h - z}{\sqrt{(z_3 + h - z)^2 + Rc^2}} - \frac{z_3 - z}{\sqrt{(z_3 - z)^2 + Rc^2}} \right] \quad (22)$$

$$q_{c4} = \frac{q_d}{2} \left[\frac{z_4 + h - z}{\sqrt{(z_4 + h - z)^2 + Rc^2}} - \frac{z_4 - z}{\sqrt{(z_4 - z)^2 + Rc^2}} \right] \quad (23)$$

z_2, z_3, z_4 being the upper side position of the three other cylinders. Finally for the Faraday pail we have:

$$q_{Fp} = \frac{q_d}{2} \left[1 - \frac{z_{Fp} - z}{\sqrt{(z_{Fp} - z)^2 + Rc^2}} \right] \quad (24)$$

But, as all the cylindrical sensors and the Faraday pail are connected together, the charge measured q_{mes} on the coulombmeter is given by:

$$q_{mes} = q_{c1} + q_{c2} + q_{c3} + q_{c4} + q_{Fp} \quad (25)$$

We can see in figure 6 an example of the theoretically measured charge during the droplet fall in terms of time using the numerical solution for the fall of the droplet and the equations 20 to 25 for the charge transferred by induction.

V. EXPERIMENTAL SETUP

It is composed of four main parts (figure 7, photograph1). The upper one is the droplet system delivery with the charging system, then a high cylinder (4.58m high and 300 mm in diameter) is used as a Faraday cage inside which are the 4 metallic cylinders (500 mm high and 150 mm in diameter) used as sensors. Finally a parallelepiped shape cage contains the collecting vessel (Faraday pail). The high cylinder was made of plastic shielded by aluminum foil; as well as the parallelepiped shape Faraday cage was made of wood shielded by aluminum foil. It is important to point out that, as the charge measured is rather weak (in the range of $10^{-10}C$), the shielding against influences of the electrical network was a major problem and could be solved more or less by consequent contact of all shielding elements and earthing them at one point. In spite of this a 50 Hz ripple could not be completely avoided (as we will see on experimental results) and manifested itself the more the lower the droplet charge was.

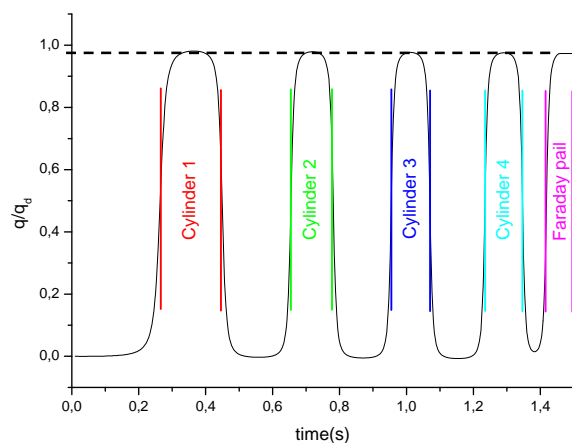


Figure 6. Example of the theoretical evolution of the charge measured during the droplet fall

A. The droplet delivery system

It is composed of a programmable syringe pump push with a stepping motor (Kd Scientific 210), a glass syringe of 20cm^3 and a needle with triple bevel (BD Microlance™ 304000) 13mm long, 0.305 mm of outer diameter and 0.140 mm of inner diameter (figure 8). With such a needle and appropriate flow rate ($0.05\text{cm}^3/\text{min}$) and also an appropriate charging voltage, we can get droplets around 1.6 – 1.7mm in diameter.

B. The droplet charging system

When the droplet is formed at the tip of the needle, it is charged by electrostatic induction with the help of a metallic ring connected to a DC high voltage, the needle being earthed (figure 7). In fact we used two DC high voltage power supplies Spellmann SL10, one +30kV 10 mA and the other -30kV 10mA, depending if we want to charge the droplets negatively or positively the droplets. The voltage applied is generally $\mp 2.5\text{ kV}$. The ring is set in a plane perpendicular to the needle which is on the ring axis at approximately 10 mm above the ring plane. Charging the droplet induces a faster detachment from the needle and thus a smaller droplet size.



Photograph1. Upper and lower part of the setup.

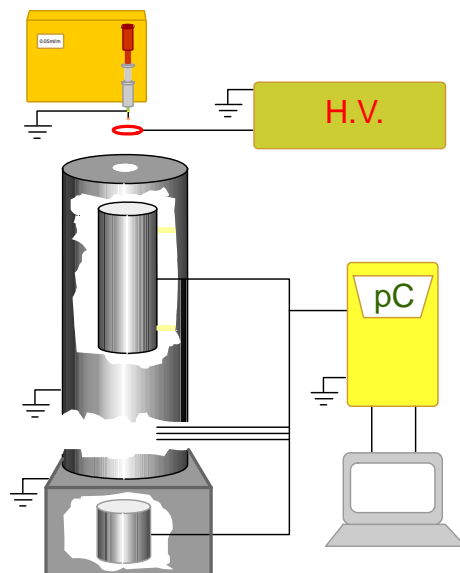


Figure 7. General setup

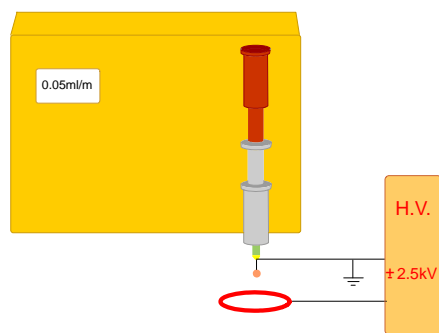


Figure 8. Droplet delivery and charging systems.

C. Sensors and collecting vessel

Four metallic cylinders are used as sensors along the droplet fall. These cylinders are fixed to the big cylinder used as a Faraday cage with two P.T.F.E. supports. The charged droplet falling on the axis of these cylinders generates a charge by electrostatic induction.

VI. EXPERIMENTS

We have tested 11 different liquids, listed in Table 1. The physical characteristics of these different liquids are in Table 1. The electrical resistivity was measured except for Ethanol-methanol for which it was too low to be measured. The other quantities are taken from data bases.

TABLE 1. Characteristics of the different liquids tested.

	Resistivity (Ωm)	Density(g/cm^3)	Kinematic viscosity (m^2/s)	Surface tension (mN/m)
Ethanol-methanol	$\leq 10^6$	0.790	$0.88 \cdot 10^{-6}$	22.
Deionized water	$\cong 10^6$	1.0	$1.0 \cdot 10^{-6}$	72.
Acetone	$1.6 \cdot 10^6$	0.791	$0.42 \cdot 10^{-6}$	23.46
Trichloethylene	$1.2 \cdot 10^9$	1.46	$0.36 \cdot 10^{-6}$	28.7
Diesel	$6.0 \cdot 10^9$	0.835	$8.4 \cdot 10^{-6}$	23.8
Kerosene	$3.2 \cdot 10^{10}$	0.793	$2.3 \cdot 10^{-6}$	23.
Toluene	$4.1 \cdot 10^{11}$	0.867	$0.68 \cdot 10^{-6}$	28.5
Heptane	$1.4 \cdot 10^{13}$	0.684	$0.6 \cdot 10^{-6}$	19.8
Essence F	$2.0 \cdot 10^{13}$	0.750	$0.9 \cdot 10^{-6}$	27.
Oil Nytro 10XN	$3.2 \cdot 10^{13}$	0.895	$28. \cdot 10^{-6}$	40.
White spirit	$4.0 \cdot 10^{14}$	0.700	$1.57 \cdot 10^{-6}$	28.

One important remark is, that, except for water and oil to a lesser extent, the surface tension of the various liquids is rather low and one could expect a breakup of the droplets [42-43] which would totally compromise our experiments. Happily, the small size of the droplets and the rather weak charge on it prevents this breakup. In fact, the position of the ring connected to the high voltage supply and as well the magnitude of the voltage have to be carefully adjusted in order to get a good droplet size and charge which will not induce a breakup but allows observing with a good accuracy the charge of the droplet during its fall.

For each liquid we made experiments for two charging voltages: -2.5 kV and +2.5 kV. As an example, we can see figures 9 and 10 the experimental results obtained with trichloethylene. These results are directly extracted from our recording from a set of experiments for each liquid and one charging polarity. It corresponds to the fall of one droplet among a set of droplets falling, this is the reason why there is an offset on time and on potential as well.

We can make several remarks. First, as this was the goal of this research, the charge on the droplet does not vary all along the fall. Indeed, the level indicated by the coulombmeter when the droplet passes the first cylinder (first summit or valley) is the same when it passes the second, the third and the fourth cylinder, except the very low drift due to the electrometer. This is the main point of all these experimental results. Second, of course, the charge on the droplet is negative when the potential on the ring is positive and positive when the applied potential is negative. Except for Toluene, for which in case of +2.5kV of charging potential the droplet sizes were greater than normal, the magnitude of the charge is often similar for both voltages applied.

We made also experiments with deionized water droplets for several applied potentials on the ring. Once more, the charge of the droplet does not vary all along its fall whatever the magnitude of its original charge was, even when the charge is very small (for no applied potential on the ring). We can see in figure 11 the evolution of the droplet charge in terms of the absolute value of the potential applied on the ring, it is nearly proportional.

In figure 12 the evolution of the droplet charge is plotted in terms of the resistivity of the liquid. Even if there is a large dispersion, it seems that the charge taken by the droplet is decreasing when the resistivity of the liquid is growing. This is probably due to the fact that the time needed for the charge transferred by induction is greater for high resistivity liquids and probably the droplet detached from the needle before the process was completed.

VII. COMPARISON BETWEEN THEORETICAL PREDICTION AND EXPERIMENTS

We are going to make this comparison in the case of kerosene. The resistivity of this liquid is in the middle range. We can see in figure 13 a comparison between the theoretical charge prediction in terms of time taking into account the numerical solution for the fall of the droplet and the equations 20 to 25 for the charge influence, with the experiments.

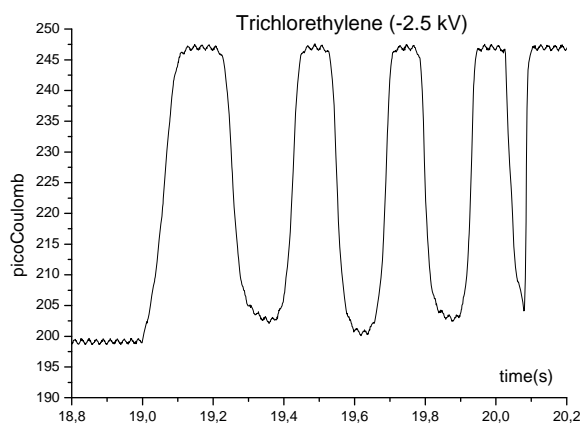


Figure 9. Trichlorethylene droplet charged with -2.5 kV

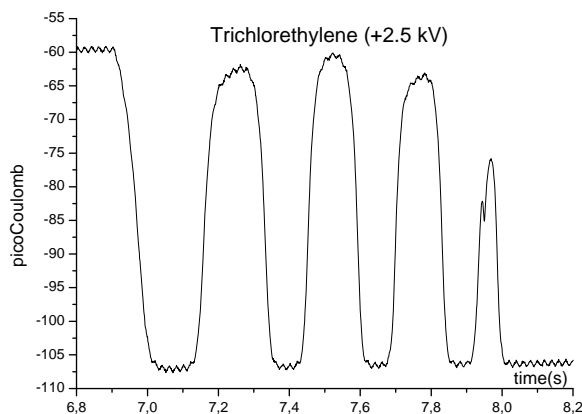


Figure 10. Trichlorethylene droplet charged with +2.5 kV

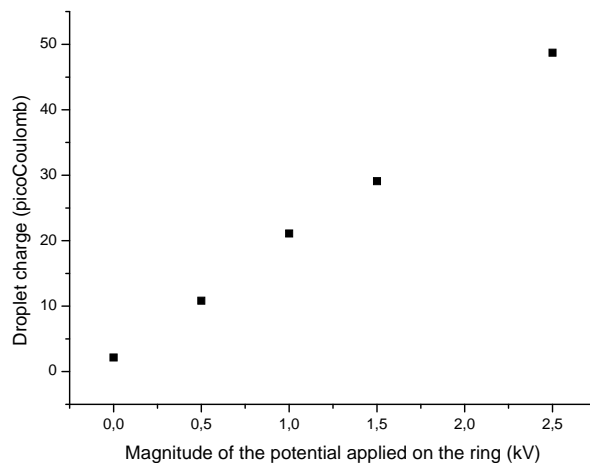


Figure 11. Water droplet charge evolution in terms of the absolute value of the potential applied on the ring

To make this comparison, the theoretical charge on the droplet has been set to the value of the droplet charge for this experiment with kerosene. The physical characteristics of the kerosene were also taken into account for the computation, and the droplet size was determined with the camera. Finally, the agreement between theory and experiment is rather good, even if the value recorded from experiments shows a slower decreasing of the charge measured when the droplet is between two successive sensors, this could be due to the electrical response of the measuring system including the electrical characteristics of sensors and cables.

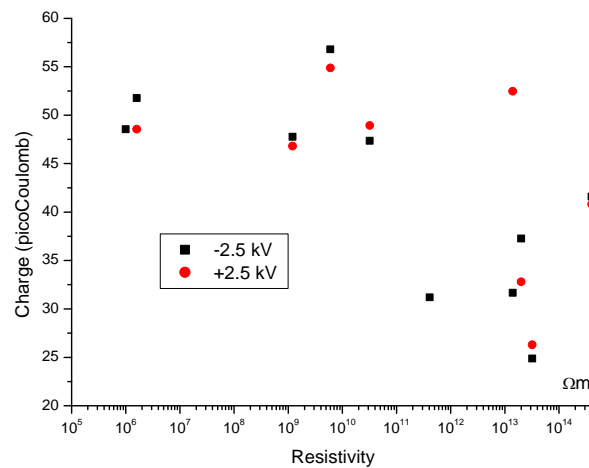


Figure 12. Evolution of the droplet charge in terms of the resistivity of the liquid

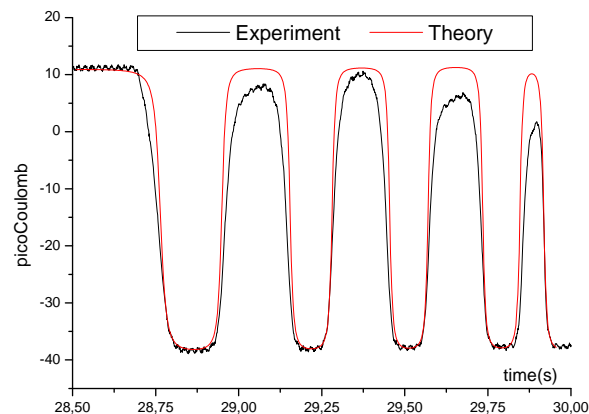


Figure 13 Comparison between theoretical prediction and experiments

VIII. CONCLUSION

The goal of this research was especially to find out if a droplet does gain charge or not during a fall in air. It has been confirmed by experiments made on 11 liquids whose electrical resistivity is distributed in a wide range that it does not. The droplet's charge, independent of its polarity, is not influenced by the fall through air. That has been proven by numerous experiments when the droplets were passing the cylinders and were collected in the pail. This does not mean that in any case falling droplets never gain charge, but the process may possibly occur during breakup and is not yet well understood.

More, we take this opportunity to make a theoretical analysis of a charged droplet falling in air on a long distance and to make a comparison with the experimental results. The rather important difference between the numerical analysis and the classical expression of a falling droplet has been pointed out and the comparison with experiments has been made using the numerical results which are more realistic. Finally the good agreement of the numerical results with the experiments seems to validate the numerical analysis.

ACKNOWLEDGEMENTS

This research was made possible by a grant from ELSTATIK Foundation (elektrostatik@elstatik.de, www.elstatik.de) (the whole results can be asked there).

REFERENCES

- [1] O. Stern "Zur Theorie der electrolytischen Doppelschicht. Z. Electrochem. 30, pp. 508-516, 1924.
- [2] G. Lüttgens, N. Wilson "Electrostatic Hazards", Butterworth Heinemann, 1997.
- [3] A. Klinkenberg, J. L. Van der Minne, Electrostatics in Petroleum Industry, (The prevention of explosion hazards), Elsevier, 1958.
- [4] A. Boumans, Streaming current in turbulent flows and metal capillaries, Physica XXIII 1007-1055, 1957.
- [5] I. Koszman, J. Gavis, Development of charges in low conductivity liquids flowing past surfaces, Chem Eng. Sci., 17, 1013-1023, 1962.
- [6] J. Gibbings, Electrostatic charging in the laminar flow in pipes of varying lengths, J. of Electroanal Chem., 25, 497-504, 1970.
- [7] H. Walmsley, G Woodford, The generation of electric currents by the laminar flow of dielectric liquids, J. Phys. D : Appl. Phys., 14, 1761-1782, 1981.
- [8] G. Touchard, P. Dumargue, "Ecoulement des liquides très faiblement conducteurs dans des tubes capillaires métalliques", C.R. Acad. Sci. ; PARIS, 270, 1041-1044, 1970.
- [9] G. Touchard, "Streaming currents developed in laminar and turbulent flows through a pipe", J. of Electrostatics, vol. 5, 463-476, 1978.
- [10] G. Touchard, M. Zahn, A. P. Washabaugh, "Relaxation charge development in plastic pipes", Inst. Phys. Conf. Ser. n° 143, 293-296, 1995.

- [11] G Touchard, T W. Patzek, C. J. Radke, "A physicochemical explanation for flow electrification in low-conductivity liquids", IEEE Trans Ind Appl, Vol. 32, n° 5, pp 1051-1057, 1996.
- [12] M. Ieda, K. Goto, H. Okubo, T. Miyamoto, H. Tskioaka and Y. Kohno, "Suppression of static electrification of insulated oil for large power transformers", IEEE Transaction on Electrical Insulation, Vol. 23, N°1, pp 153-157, 1988.
- [13] M.J. Lee, J.K. Nelson and M.A. Franchek, "Electrification in transformer model structures", EPRI Workshop Proceedings, Static Electrification in Power Transformers, EPRI EL-6918, 1990.
- [14] T. Miyamoto, A. Kishi, Y. Miura, "Effect of Insulating Oils Streaming Electrification in Transformers", EPRI EL-6918, 1990.
- [15] A.J. Morin, M Zahn, J Melcher, "Fluid electrification measurements of transformer pressboard/oil insulation in a Couette Charger using an absolute charge sensor", IEEE Transactions on Electrical Insulation, Vol. 26, No. 5, pp. 870-901, 1991.
- [16] H. Romat, G. Touchard, O. Moreau, "Flow Electrification in Power Transformers" EPRI Workshop Proceeding Static electrification in Power Transformers, 1994.
- [17] A. Washabaugh, M.Zahn, A study of the effect of BTA on flow electrification using rotating cylindrical electrodes, EPRI Workshop Proceedings: Static electrification in Power Transformers, 1994.
- [18] M. A. Brubaker, J. K. Nelson, "A full scale simulation of streaming electrification effects in a large scale core-form transformer winding", EPRI TR-105019, 1995.
- [19] G. Artana, G. Touchard, O. Moreau, "Flow electrification due to the flow of a perpendicular jet on a flat plate", Journal of Electrostatics, 41, pp129-134, 1997.
- [20] T. Paillat, E. Moreau, G. Touchard, "Flow electrification through porous media", Inst. Phys. Conf. Ser. n° 163, 229-232, 1999.
- [21] T. Paillat, E. Moreau, G. Touchard, "Flow electrification through Porous media", Journal of Loss Prevention in the Process Industries Vol. 14, 91-93, 2001.
- [22] E. Moreau, T. Paillat, G. Touchard, "Space charge density in dielectric and conductive liquids flowing through a glass pipe", Journal of Electrostatics, Vol. 50-51, 448-454, 2001.
- [23] T. Paillat, E. Moreau, G. Touchard, "Space charge density at the wall in the case of heptane flowing through an insulating pipe", Journal of Electrostatics, Vol. 53, Issue 2, 171-182, 2001.
- [24] G. Touchard, "Flow electrification of liquids ", Journal of Electrostatics, Vol. 50-51, 440-447, 2001.
- [25] O. Moreau, G. Touchard, "Experimental study and modeling of static electrification in power transformer", IEEE Transactions on Industry Applications, Vol. 37, 971-977, 2001.
- [26] E. Moreau, T. Paillat, G. Touchard, "Flow electrification in high power transformers : BTA effect on pressboard degraded by electrical discharges", IEEE Transactions on Dielectrics and Electrical Insulation, vol. 10, 15-21, 2003.
- [27] O. Moreau, T. Paillat, G. Touchard, "Flow electrification in transformers : Sensor prototype for electrostatic hazard", Inst. Phys. Conf. Ser., N. 178, 31-37, 2004.
- [28] J. Vazquez-Garcia, J. Rivenc, A. Agneray, T. Paillat, G. Touchard, "A critical approach to measure streaming current : case of fuel flowing through conductive and insulating polymers pipes", IEEE Transactions on Industry Applications. vol 41, pp 1335-1342, 2005.
- [29] F. Perisse, J. Vazquez-Garcia, T. Paillat, G. Touchard, "Fuel electrification: moisture and temperature influence", Journal of Electrostatic, vol 63, pp 481-487, 2005.
- [30] A. Bourgeois, T. Paillat, G. Mortha, O. Moreau, G. Touchard, "Flow electrification in power transformers : salts-type additive as a potential remedy", Journal of Electrostatic, Vol. 63, page 877-882, 2005.
- [31] J. Vazquez-Garcia, J. Rivenc, A. Agneray, T. Paillat, G. Touchard, "A critical approach to measure streaming current : case of fuel flowing through conductive and insulating polymers pipes", IEEE Transactions on Industry Applications Vol. 41, pp. 1335-1342, 2005.
- [32] A. Bourgeois, G. Mortha, T. Paillat, G. Touchard, O. Moreau, Y. Bertrand, "Flow electrification in power transformers: Study of potential remedy", IEEE Transactions on Dielectric and Electrical Insulation. Vol. 13, No 3, pp. 650-656, 2005.
- [33] T. Paillat, O. Moreau, J.M. Cabaleiro, F. Perisse, G. Touchard, "Electrification par écoulement modélisation électrique", Journal of Electrostatic, vol. 64, pp. 485-491, 2006.
- [34] J. M. Cabaleiro, T. Paillat, O. Moreau, G. Touchard, "Flow electrification of dielectric liquids in insulating channels: limits to the application of the classical wall current expression", Journal of Electrostatic, vol 66, page 79-83, 2007.
- [35] J. M. Cabaleiro, T. Paillat, O. Moreau, G. Touchard, "Electrical double layer's development analysis : Application to flow electrification in power transformers ", IEEE Transaction on Industry Applications, vol 45, pp. 597-605, 2009.
- [36] T. Paillat, G. Touchard, "Electrical charges and liquid motion", Journal of Electrostatic Vol. 67, pp. 326-334, 2009
- [37] M. El-Adawy, J. M. Cabaleiro, T. Paillat, O. Moreau, G. Touchard, "Physicochemical Analysis at the Interface Between Conductive Solid and Dielectric Liquid for Flow Electrification Phenomenon", IEEE Transaction on Industry Application, Vol. 46, pages 1593-1600 , 2010.
- [38] T. Paillat, C. Perrier, Y. Zelu, G. Morin, "Ester oils and flow electrification hazards in power transformers", IEEE Transactions on Dielectrics and Electrical Insulation, Vol. 19, Issue 5, pp. 1537-1543, 2012.
- [39] T. Paillat, G. Touchard, " "Capacitive sensor" to measure flow electrification and prevent electrostatic hazards ", Sensors 2012, 12, doi:10.3390/s121114315, pp. 14315-14326, 2012.
- [40] M. Benmadda, G. Touchard, "Charges électriques engendrées par un écoulement de gaz empoussiéré dans une conduite métallique (étude théorique et expérimentale)", Journal of electrostatics, vol. 15, n °3, 307-314, 1984.
- [41] H. Schlichting "Boundary layer theory", Mc Graw-Hill, 1960.
- [42] E. Villiermaux and B. Bossa, "Single-drop fragmentation determines size distribution of raindrops", Nature Physics, DOI:10.1038/NPHYS1340, 2009.
- [43] M.-J. Ni, S. Komori, N. B. Morley, "Direct simulation of falling droplet in a closed channel", International Journal of Heat and Mass Transfer, 49, 366-376, 2006.